# Identification and characterization of the intercellular adhesion molecule-2 gene as a novel p53 target

## Supplementary Materials

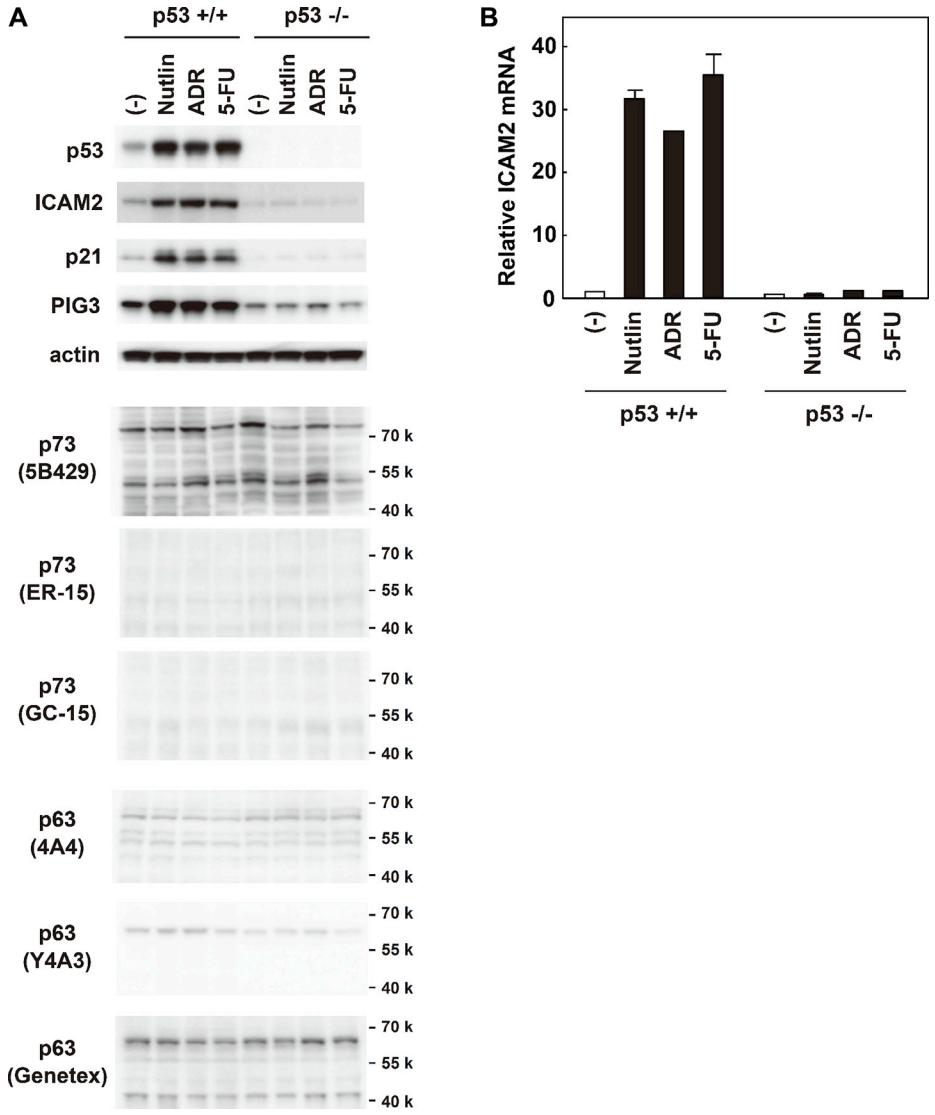


**Supplementary Figure S1: Endogenous p53 upregulates ICAM2 protein and mRNA levels.** (**A**) HCT116-p53(+/+) and HCT116-p53(−/−) cells were treated with 0.5 μg/mL ADR, 20 μg/mL 5-FU, or 10 μM Nutlin-3 for 24 h. Immunoblot analyses of ICAM2, p53, p21, PIG3, β-actin, p73, and p63 were conducted. The primary antibodies used for p73/p63 immunoblot are as follows: mouse anti-human p73 monoclonal antibody (mAb) (5B429, (Santa Cruz Biotechnology), ER-15 (Oncogene Research), and GC-15 (Oncogene Research)); mouse anti-human p63 mAb (4A4 (Santa Cruz Biotechnology) and Y4A3 (Thermo Scientific)); rabbit anti-human p63 polyclonal Ab (N2C1, Genetex Inc.). (**B**) Cells were treated as described above, and *ICAM2* mRNA levels were assayed by real-time RT-PCR. Relative gene expression levels were quantified using the ΔΔCt method and the results were normalized to the expression of the *GAPDH* gene. The data are shown as the mean ± standard errors of 3 independent experiments and were normalized to their respective controls as 1.

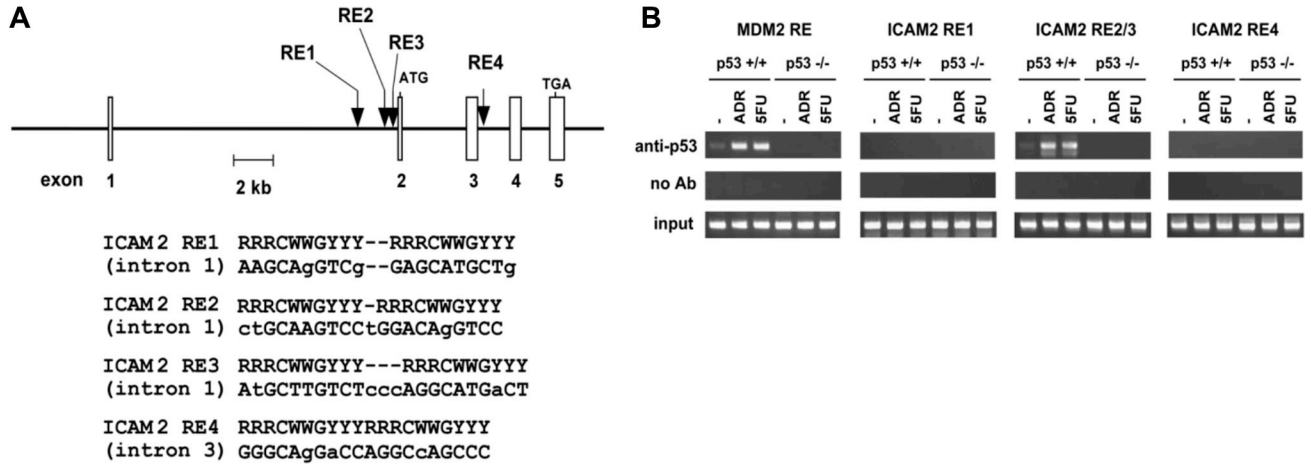


**Supplementary Figure S2: Potential responsive sites in the *ICAM2* gene.** (**A**) The position and nucleotide sequence of candidate response elements for p53 family in the *ICAM2* gene. The consensus sequences are indicated by upper-case letters and the spacer sequences between 10-bp motifs are indicated by -. Lower-case letters identify mismatches with the consensus sequence. R represents purine; Y, pyramidine; W, adenine or thymine. (**B**) HCT116-p53(+/+) and HCT116-p53(−/−) cells were treated with 0.5 μg/mL ADR or 20 μg/mL 5-FU for 24 h and subjected to ChIP assay in the presence of p53 protein at candidate binding sites and the *MDM2* promoter. Oligonucleotide primer sequences are as follows: ICAM2 RE1 sense 5′-GCGACACTTCAACCTTCTTGCC-3′, ICAM2 RE1 antisense 5′-CCCTGCCTCCCTGAGCTCCT-3′; ICAM2 RE2/3 sense 5′-TGCGTGTATGAGACGTGTGCA-3′, ICAM2 RE2/3 antisense 5′-AGCCTGGGCGACAAGAGTGAG-3′; ICAM2 RE4 sense 5′-GGTGCCCACCACCTTGCATAC-3′, ICAM2 RE4 antisense 5′-GGGTCCTTCAGACCAGCCTGC-3′; and *MDM2* promoter sense 5′- GTTCAGTGGGCAGGTTGACT-3′, *MDM2* promoter antisense 5′- GCTACAAGCAAGTCGGTGCT-3′. To ensure that PCR amplification was performed in the linear range, template DNA was amplified for a maximum of 40 cycles.

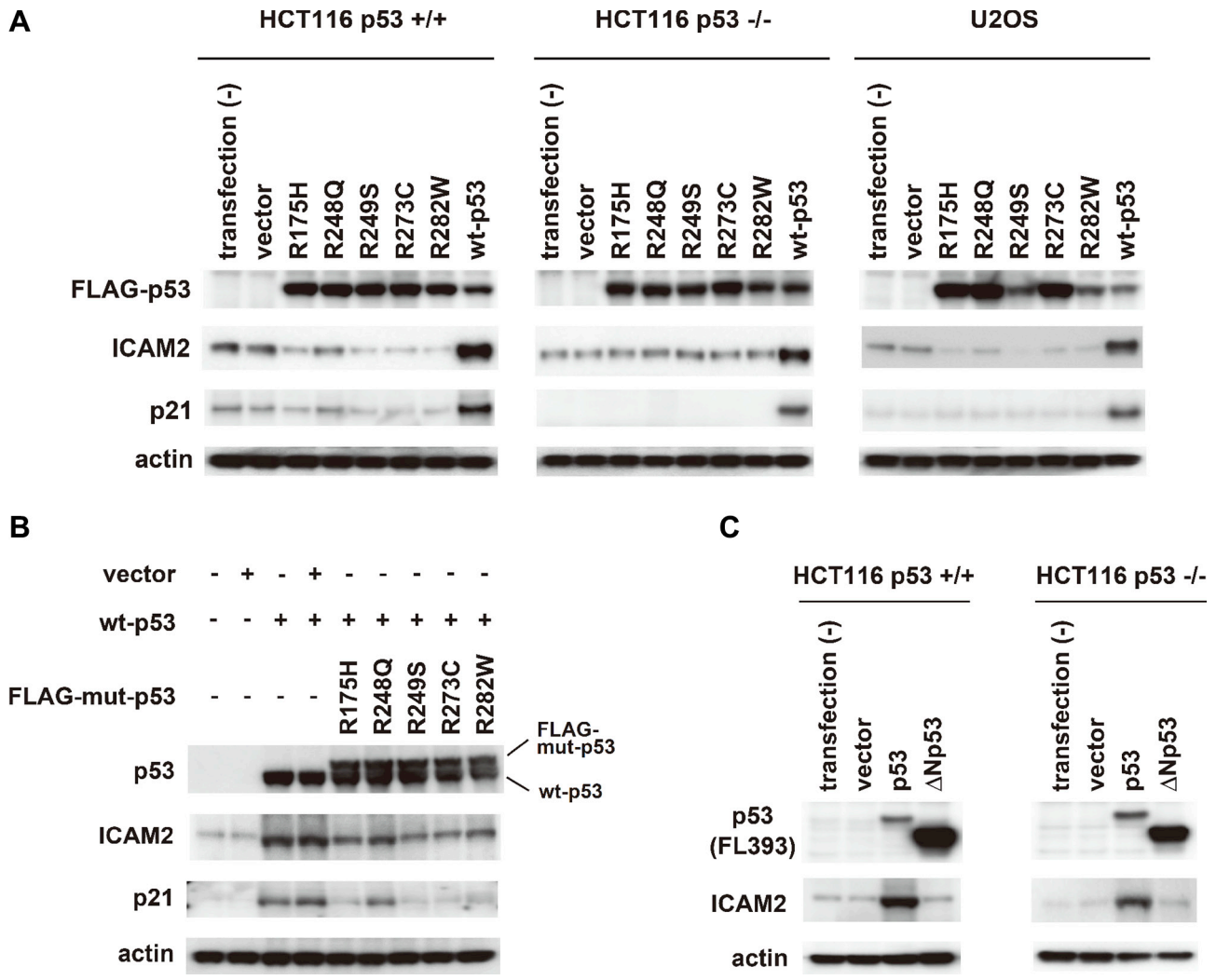


**Supplementary Figure S3: The effect of mutant-p53 and ΔNp53 on ICAM2 expression.** (**A**) Cells were transfected with various mutant p53–expressing plasmids or a wild-type p53-expressing plasmid. Cells were harvested 48 h after transfection, and immunoblot analysis was performed using an anti-ICAM2 Ab. p53 mutant constructs encoding p53 mutants commonly seen in human cancers (R175H R248Q, R249S, R273C, and R282W) were generated by subcloning into the pcDNA3.2 plasmid with an N-terminal FLAG epitope tag (Invitrogen). (**B**) HCT116-p53(−/−) cells were transfected with empty or FLAG-tagged mutant-p53-expressing vectors. After 8 h, cells were then transfected with wt-p53-expressing plasmid (no FLAG) for 24 h. ICAM2 induction by ectopic expression of wild-type p53 was partially reversed by all p53 mutants, indicating that certain p53 mutants indeed have a dominant negative effect against exogenous p53 on the regulation of ICAM2. (**C**) HCT116-p53(+/+) and HCT116-p53(−/−) cells were transfected with empty, wild-type p53-, or ΔNp53 (Δ40p53α)-expressing vectors and were harvested 24 h after transfection.ICAM2 and p53 protein levels were determined by immunoblot analysis . p53 immunoblot was performed using the rabbit anti-human p53 polyclonal Ab (FL393, Santa Cruz Biotechnology), which recognizes amino acids 1-393 of human p53. A ΔNp53 construct was generated by subcloning into the pF5K-CMV-neo plasmid (Promega).

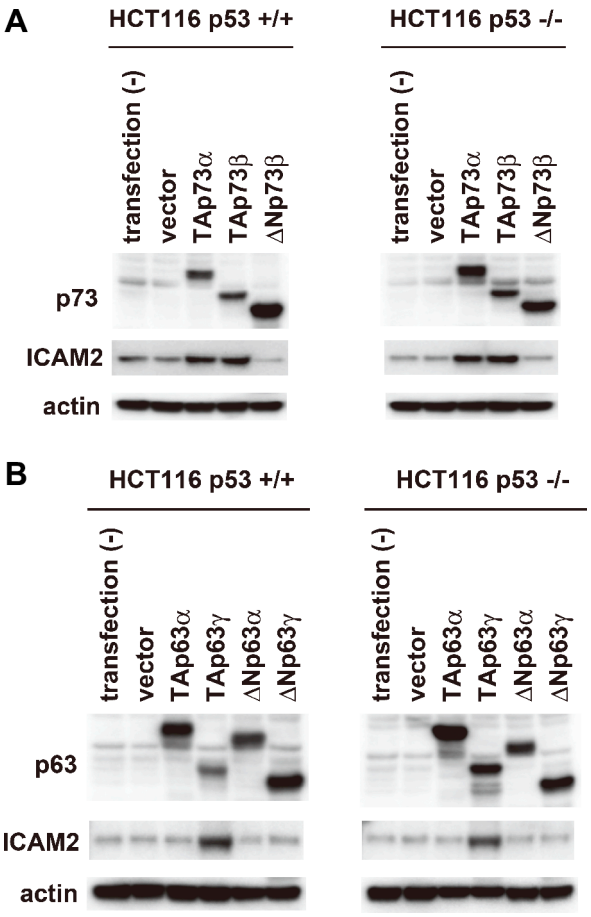


**Supplementary Figure S4: The effect of ΔNp73 (A) and ΔNp63 (B) on ICAM2 expression.** All ΔNp73/p63 constructs were generated by subcloning into the pF5K-CMV-neo plasmid. HCT116-p53(+/+) and HCT116-p53(−/−) cells were transfected with empty or p73/p63-expressing vectors for 24 h. ICAM2 protein levels were determined by immunoblot analysis.

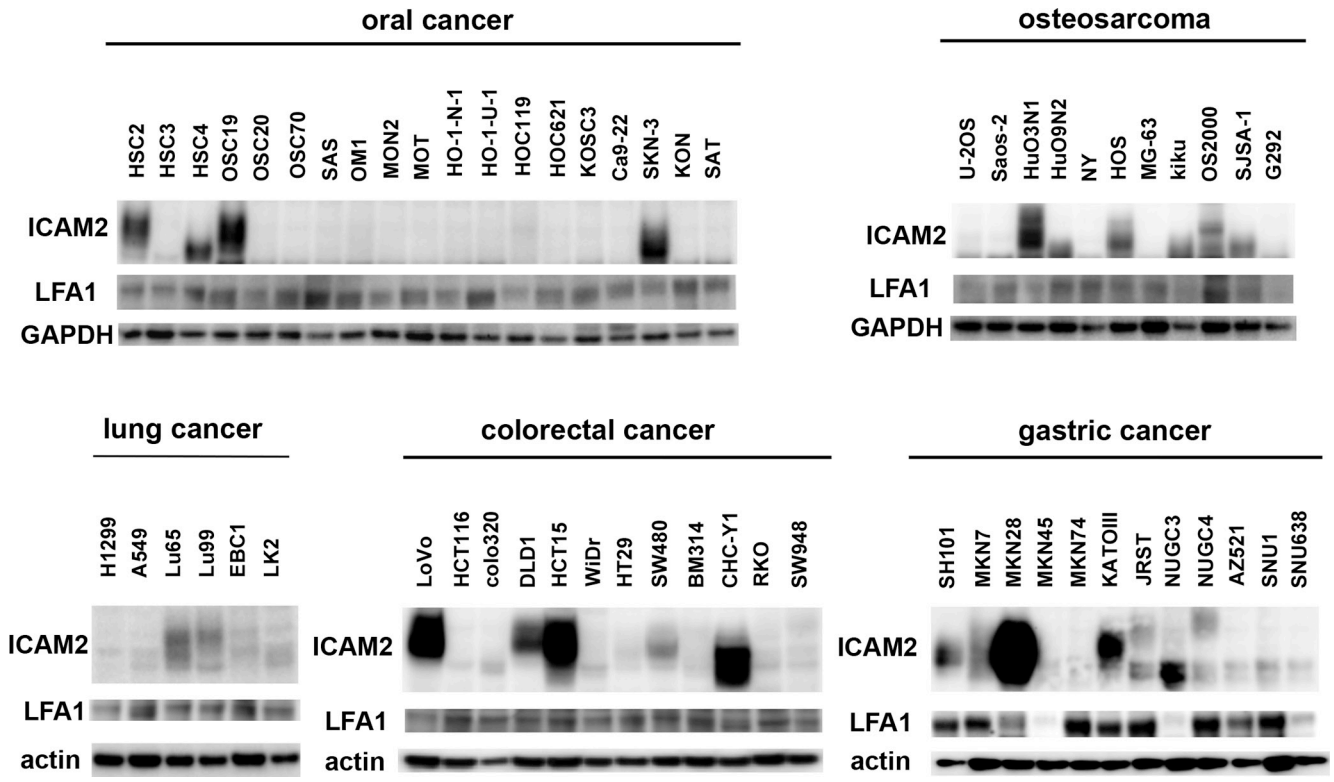


**Supplementary Figure S5: Expression of endogenous ICAM2 and LFA1 in human cancer cell lines.** Immunoblot analysis was performed using anti-ICAM2 and anti-LFA1 (CTB-104; Santa Cruz Biotechnology) antibodies. The endogenous p53 statuses in these cell lines are follows: Wild-type: U-2OS, HuO9N2, NY, MG-63, kiku, OS2000, SJSA-1, A549, Lu99, LoVo, HCT116, CHC-Y1, RKO, JRST, NUGC4, AZ521 and SNU1. Wt/mut: MKN45 Large deletion: Saos2, H1299 and KATOIII. Mutant-type: HSC2, HSC3, HSC4, OSC19, OSC20, OSC70, SAS, OM1, MON2, MOT, HO-1-N1, HO-1-U1, HOC119, HOC621, KOSC3, Ca9-22, SKN3, KON, SAT, HuO3N1, HOS, G-292, Lu65, EBC1, LK2, colo320, DLD1, HCT15, WiDr, HT29, SW480, BM314, SW948, SH101P4, MKN7, MKN28, MKN74, NUGC3 and SNU638. Data were from the IARC TP53 Database (http://p53.iarc.fr/CellLines.aspx), or we originally examined genetic alterations in exons 2 through 11 of the p53 gene (Oshima et al. Antitumor effect of adenovirus-mediated p53 family gene transfer on osteosarcoma cell lines. Cancer Biol Ther 2007; 6:1058–1066; Kusano et al. Genetic, epigenetic, and clinicopathologic features of gastric carcinomas with the CpG island methylator phenotype and an association with Epstein-Barr virus. Cancer 2006; 106:1467–1479; our unpublished data). Additionally, we performed a multigene sequencing screen interrogating 2855 mutational hotspots in 50 cancer-related genes using the AmpliSeq Cancer Hotspot Panel v2 and Ion Torrent semiconductor sequencer. This panel can explore hotspot regions of the following 50 cancer-associated genes: ABL1, AKT1, ALK, APC, ATM, BRAF, CDH1, CDKN2A, CSF1R, CTNNB1, EGFR, ERBB2, ERBB4, EZH2, FBXW7, FGFR1, FGFR2, FGFR3, FLT3, GNA11, GNAS, GNAQ, HNF1A, HRAS, JAK2, JAK3, IDH1, IDH2, KDR/ VEGFR2, KIT, KRAS, MET, MLH1, MPL, NOTCH1, NPM1, NRAS, PDGFRA, PIK3CA, PTEN, PTPN11, RB1, RET, SMAD4, SMARCB1, SMO, SRC, STK11, TP53, VHL. Library preparation and sequencing with an Ion Torrent PGM was performed as previously described (J Mol Diagn. 2013; 5:607–22). Approximately 800X average coverage was obtained with > 98% of target bases having at least 100 sequence reads. Alignment to the hg19 genome and variant calling was performed by Ion Reporter Software 4.0.

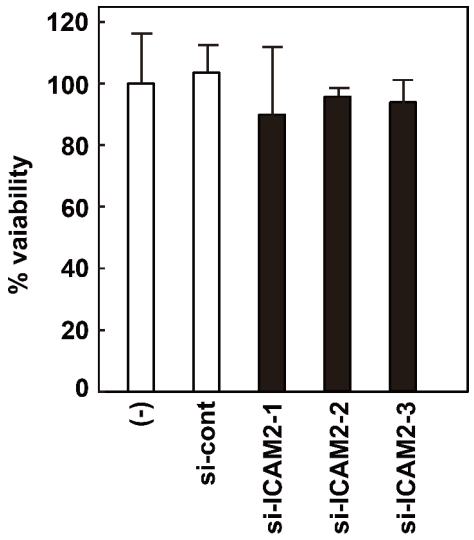


**Supplementary Figure S6: ICAM2 silencing does not inhibit cancer cell growth.** Expression of ICAM2 in HSC4 cells was silenced as described in the text. Cell viability was assessed by the uptake of tritium thymidine using a 3-(4,5-dimethylthiazol-2-yl)-2,5-diphenyltetrazolium bromide (MTT) assay. The assay was performed in triplicate with a Cell Counting Kit-8 (Dojindo, Tokyo, Japan) according to the manufacturer's instructions. Error bars equal one standard error.

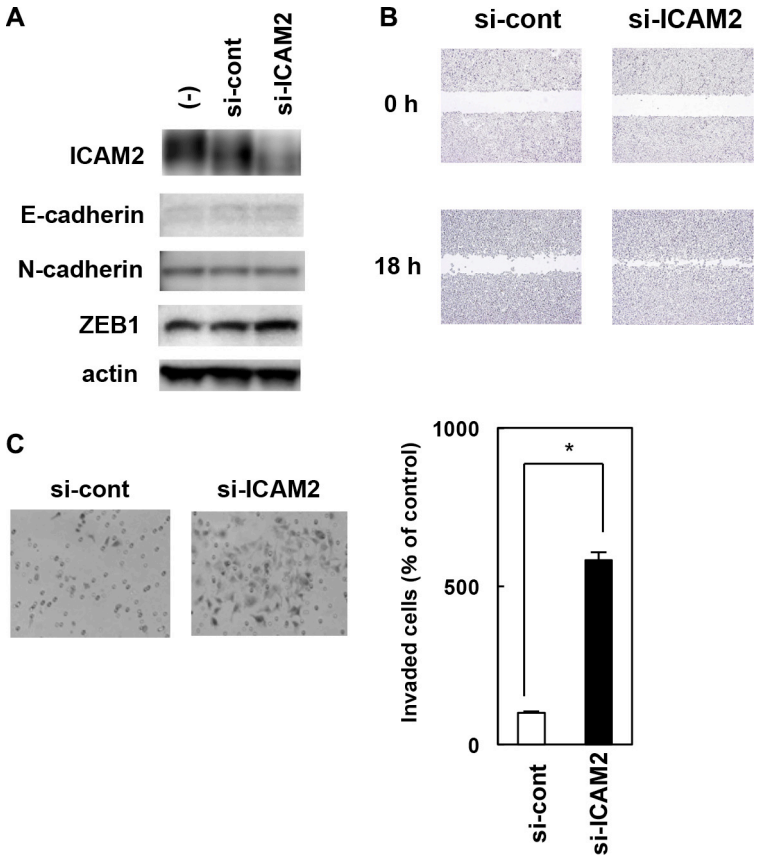


**Supplementary Figure S7: Silencing of ICAM2 by siRNA vector promotes migration and invasion of CHC-Y1 cells.** (**A**) Immunoblot analysis after stable transfection of ICAM2 siRNA plasmid (si-ICAM2) or empty plasmid (si-cont) in CHC-Y1 colon cancer cells. (**B**) Wound healing assay of ICAM2 siRNA plasmid-transfected cells. Phase contrast images were taken at 0 and 18 h after wounding. (**C**) Cell invasion was measured in a Matrigel invasion assay following stable transduction. The experiments were repeated three times with similar results. Representative images showed increased cell invasion in ICAM2 siRNA-transfected CHC-Y1 cells (left). Quantification of invasion as a percentage of the control is also shown (right). Asterisk, significant differences (*$p < 0.01$; relative to empty vector (si-cont)).

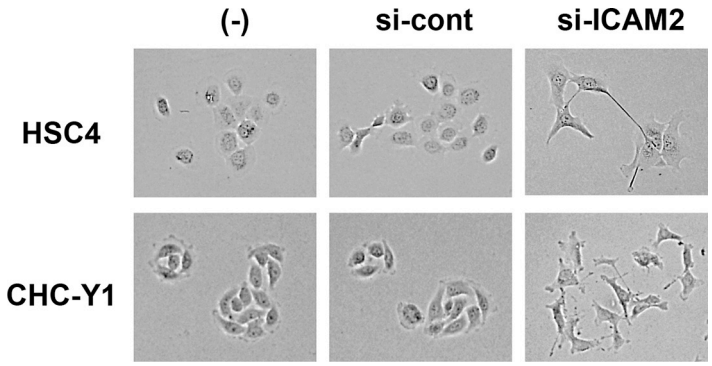


**Supplementary Figure S8: Morphology analysis of HSC4 and CHC-Y1 cells following silencing of ICAM2 by siRNA vector.** Photographs were taken under a phase-contrast microscope, showing that ICAM2-knockdown cells acquired a spindle cell type morphology with projections, and the number of cell-cell contacts was reduced.

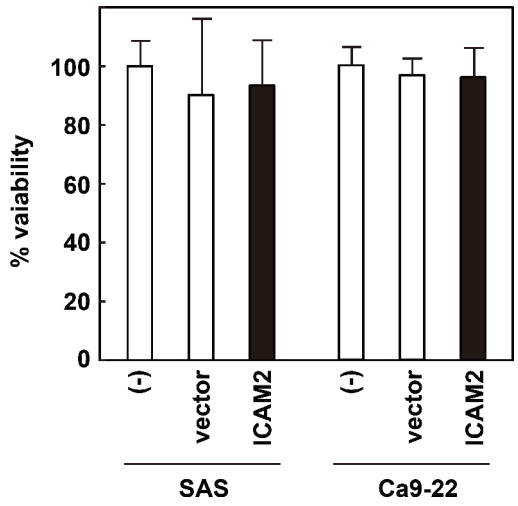


**Supplementary Figure S9: Overexpression of ICAM2 does not inhibit cancer cell growth.** SAS and Ca9-22 cells were stably transfected with ICAM2 expression vector or empty vector plasmid (vector). Cell viability was assessed by MTT assay. Error bars equal one standard error.

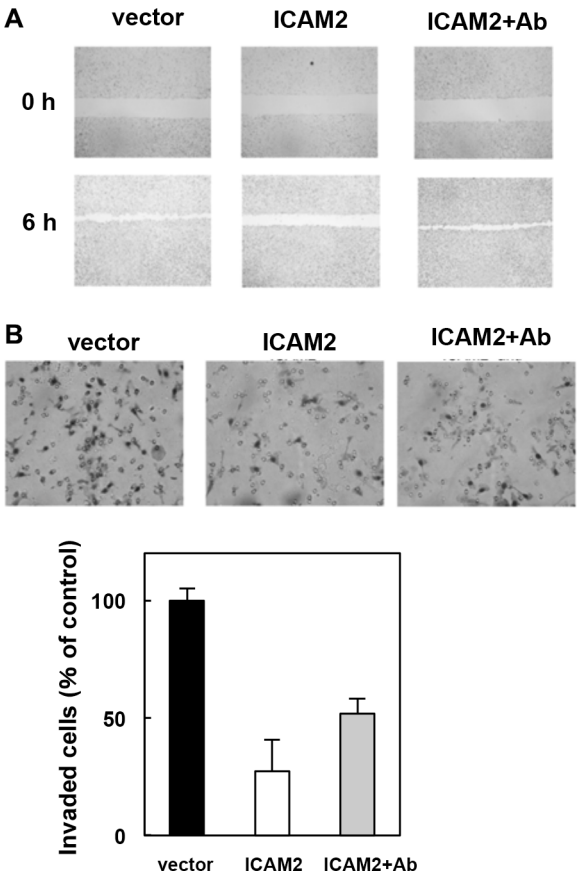


**Supplementary Figure S10: ICAM2-mediated inhibition of cancer cell migration and invasion was blocked by anti-ICAM2 antibody.** (**A**) The migration-inhibiting effect of ICAM2 was blocked by the addition of anti-ICAM2 Ab. Control and ICAM2-transfected Ca9-22 cell monolayers were scratched manually with a plastic pipette tip. Cells were washed with fresh medium to remove floating cells and cultured with or without anti-ICAM2 Ab (1.25 μg/mL). Wound healing was monitored 6 h after wounding. (**B**) The invasion-inhibiting effect of ICAM2 was blocked by the addition of anti-ICAM2 Ab. Control and ICAM2-transfected Ca9-22 cells were subjected to invasion assays. When necessary, an anti-ICAM2 Ab (1.25 μg/mL) was added to the medium. The experiments were performed in triplicates. Quantification of invasion as a percentage of the control is shown (lower panels).

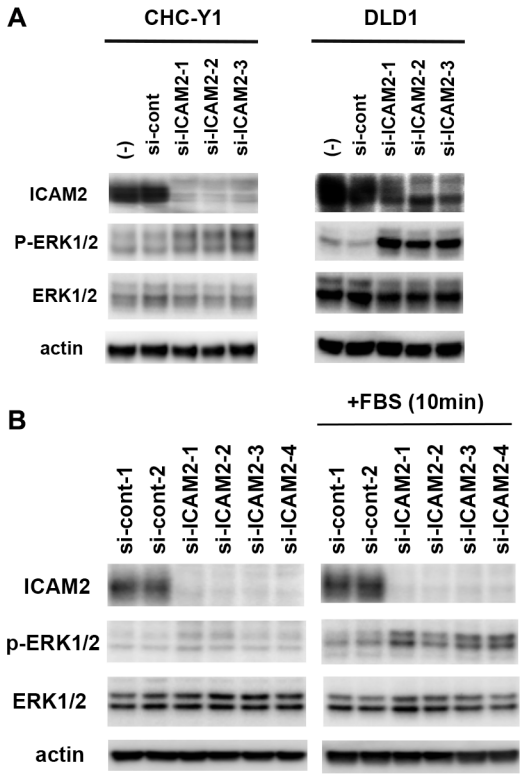


**Supplementary Figure S11: ICAM2 siRNA enhanced ERK1/2 phosphorylation in cancer cells.** (**A**) After stable transfection of ICAM2 siRNA plasmid (3 populations, si-ICAM2-1, 2, and 3) or empty plasmid (si-cont) in CHCY1 and DLD1 colorectal cancer cells, cell lysates (20 μg of protein) were subjected to immunoblot with antibodies against p- ERK1/2, ERK1/2, and β-actin. (**B**) HCT15 colorectal cells were stably transfected with ICAM2 siRNA plasmid (4 populations, si-ICAM2-1, 2, 3, and 4) or empty control plasmid (2 populations, si-cont-1 and 2). Cells were also serum-starved overnight, followed by FBS stimulation (10%, 10 min, right panel). Inhibition of ICAM2 expression by siRNA enhanced FBS-induced phosphorylation of ERK.

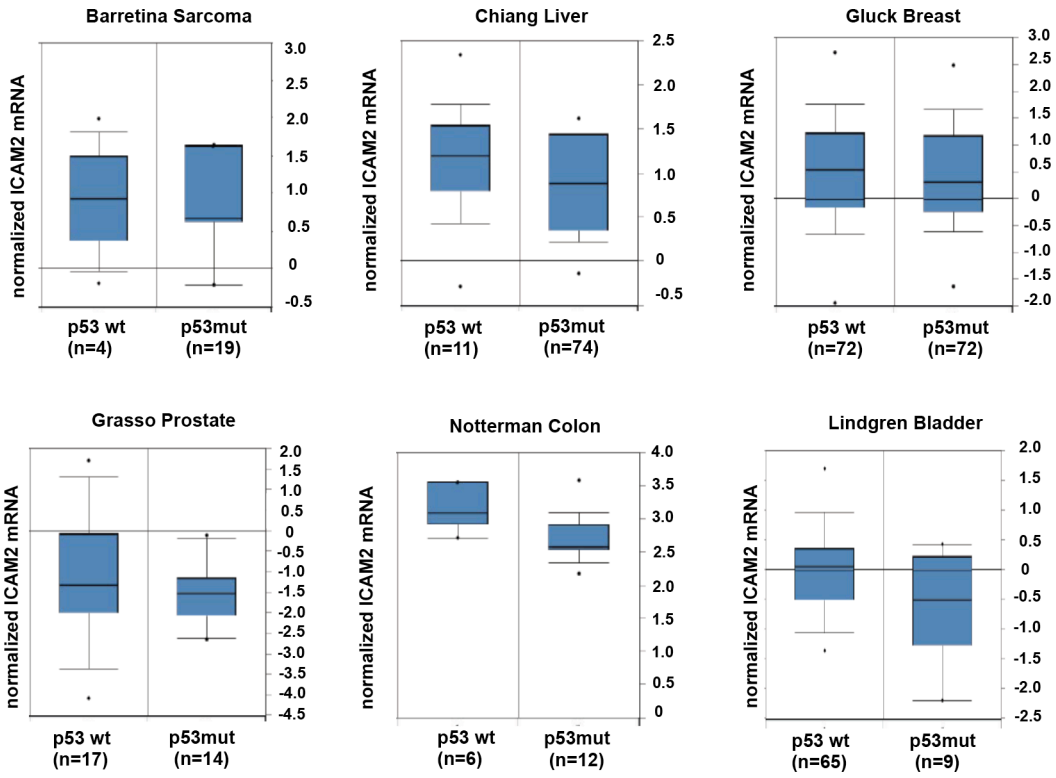


**Supplementary Figure S12: *ICAM2* expression profiles in human tumors using published human oncology microarray data, Oncomine.** Left bars, *ICAM2* expression in tumors with wild-type p53 ; right bars, *ICAM2* expression in tumors with mutant p53. Data are displayed as a boxplot (log2 median-centered) according to Oncomine output.

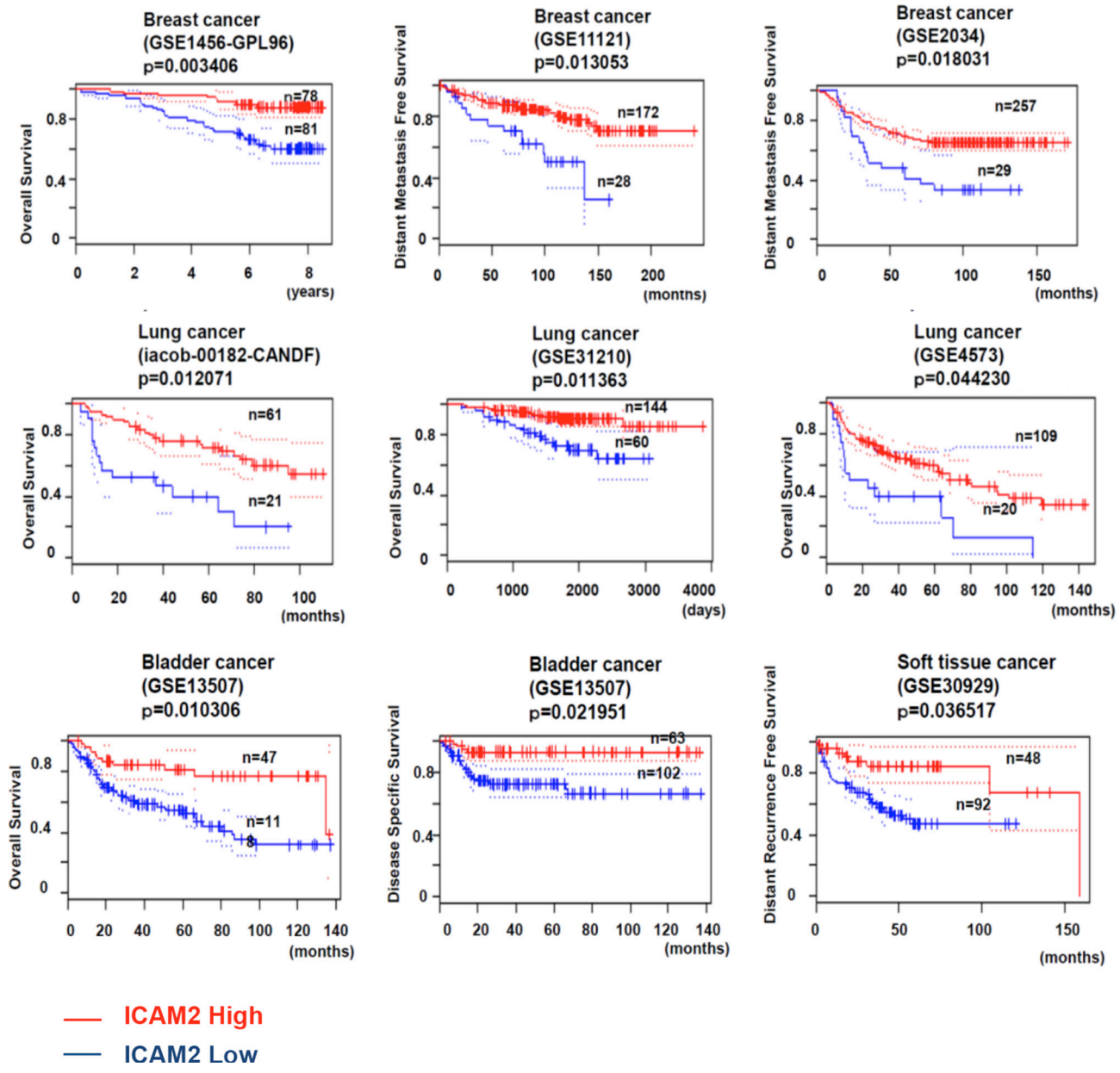


**Supplementary Figure S13: The correlation between *ICAM2* expression and prognosis among cancer patients.** Relationship between the expression of *ICAM2* and prognosis in cancer patients was examined using the PrognoScan database.